Wetting-induced budding of vesicles in contact with several aqueous phases

Supplementary Information

*Yanhong Li, Halim Kusumaatmaja, Reinhard Lipowsky, Rumiana Dimova**

Max Planck Institute of Colloids and Interfaces, Science Park Golm, 14424 Potsdam, Germany

* Address correspondence to: dimova@mpikg.mpg.de

Materials: Poly(ethylene glycol) or PEG (average molecular weight 8000 g/mol) and dextran from Leuconostoc mesenteroides (molecular weight between 400 kDa and 500 kDa) were purchased from Sigma-Aldrich. The polydispersity, measured with gel permeation chromatography, was 1.11 for PEG and 1.83 for dextran. Sucrose was purchased from Fluka. Lipids including 1,2-dioleoyl-sn-glycero-3-phosphatidylcholine (DOPC), and 1,2-dipalmitoyl-sn-glycero-3-phosphatidylethanolamine-N-(lissamine rhodamine B sulfonyl) as chloroform solutions and galbeta1-3galnacbeta1-4(neuacalpha2-3)galbeta1-4glcbeta1-1'-cer (G_{M1} Ganglioside) as powder were purchased from Avanti Polar Lipids. In some occasions, instead of G_{M1} we used membranes containing 4% dioleoylphosphatidylethanolamine-N-[methoxy (polyethylene glycol)-2000] (ammonium salt) (DOPE-PEG2000); data not shown. G_{M1} and DOPE-PEG2000 were added in order to tune the interaction of the membrane with one of the two aqueous phases enclosed in the vesicles. Since the headgroup of G_{M1} consists of sugar moieties, it is

expected to induce stronger interactions of the membrane with the dextran-rich phase, while DOPE-PEG2000 is expected to interact stronger with the PEG-rich phase.

Giant vesicle preparation using electroformation: Lipid stock solution in chloroform (25~30 µl, 2 mg/ml) was spread on conductive glass substrates coated with indium tin oxide (ITO). The lipid films were dried in a vacuum desiccator for at least 3 hours. A rectangular Teflon frame of thickness 1.6 mm served as a chamber spacer between two opposing glass substrates. The chamber was sealed with grease. The coated ITO surfaces acted as electrodes. Approximately 2 ml polymer solution was injected into the chamber through a 0.22 µm filter. The chamber, the filter, the injection syringe, the needle and the polymer solution were preheated at 60 ºC in an oven. The filled chamber was placed in the oven at 60 ºC, and immediately afterwards, an AC field of 1.5 ~ 2.2 V (peak-to-peak, according to the resistance of the ITO glasses) and 10 Hz was applied using a function generator (Agilent 33220A 20MHz function/arbitrary waveform generator). The electroformation continued for 2 or 3 hours. The vesicles were prepared at 60 ºC to ensure homogeneity of the polymer solution. After the formation, the chamber was cooled to room temperature and the vesicle solution was transferred into a small tube.

Phase diagram of the polymer aqueous solution: The binodal of the PEG and dextran aqueous solution at room temperature was determined by cloud-point titration for each polymer concentration combination; see Fig. S1. At first, concentrated PEG and dextran aqueous stock solutions were prepared. The mass of a small well-sealed vial with a stirring bar inside was measured with a balance (Mettler AT261 DeltaRange). Then, a certain amount of the dextran stock solution and water was injected inside, and the added weight measured. The PEG stock solution was injected drop-wise under stirring until the solution in the vial became turbid and the added weight was measured again. The same procedure was repeated for several different initial dextran concentrations. The cloud point titration was done at 23ºC.

Note that the molecular weight and the polydispersity of the polymers can influence the binodal. In a similar fashion, the vesicle behavior is very sensitive to the concentration of the polymer solutions.

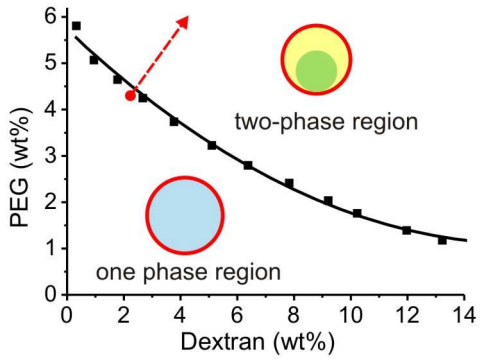

Figure S1. Phase diagram of the PEG-dextran polymer solution at 23ºC. The black squares indicate the binodal measured at 23ºC (the solid line is a guide to the eye). Below the binodal the polymer solution is homogeneous; above the binodal it phase separates. The red dashed line indicates the experimental trajectory of the deflation of vesicles initially loaded with the polymer solution (red dot: 4.05% PEG, 2.22% dextran). The insets schematically illustrate the vesicle membrane (red) enclosing the homogeneous solution (blue) or the two separated phases, dextran-rich (green) and PEG-rich (yellow).

Batch measurements on deflated vesicles: We performed deflation measurements on populations of vesicles, which are initially spherical. After deflation the vesicles change their morphology to a budded state and the intrinsic contact angle for all vesicles is the same. The morphological change after this single-step deflation was examined on altogether 64 vesicles. Since the preparation procedure of electroformation produces vesicles with different initial excess areas (or membrane tensions) and different volumes, each vesicle in the batch reaches a different degree of budding after the deflation step. Some examples are given in Fig. S2.

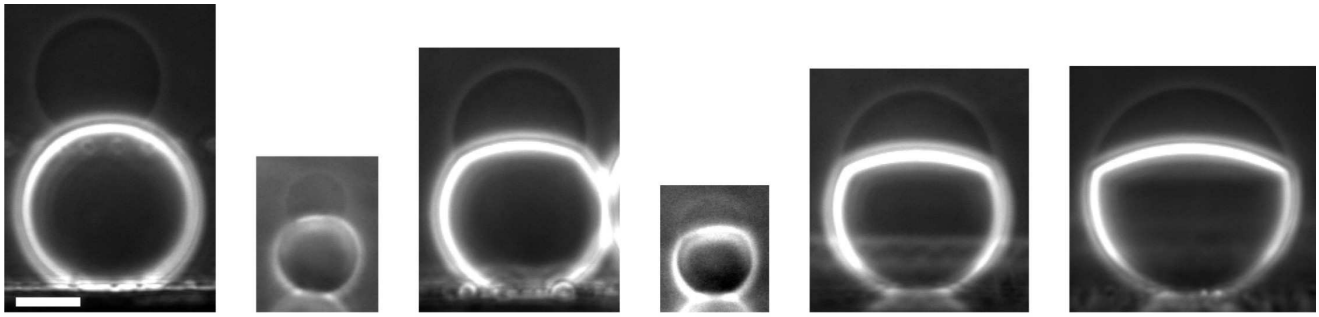

Figure S2. Phase contrast images (side view observation) of different vesicles after a single-step deflation. The lower droplet consists of the heavier dextran-rich phase, the upper droplet of the lighter PEG-rich phase. All images have the same magnification. The scale bar in the first snapshot corresponds to 20 μm.

Force balance and intrinsic contact angle for inward budding: In the main text, the outward budding process was analyzed using force balance arguments in analogy to Neumann's triangle for capillary surfaces. In the following, we will discuss the process of inward budding. In the experimental system, see Fig. 1(g, h), both the internal medium and the external continuous media (black regions) are PEG-rich phases. For clarity, we denote the inner medium by *i*, and the external one by *p*; the dextran-rich phase is denoted by *d*. Furthermore, we define the three contact angles, θ_i, θ_p, and θ_d, see Fig. S3a, obtained from the microscopy images. At the contact line, the membrane tensions $\hat{\Sigma}_{pi}$ and $\hat{\Sigma}_{di}$, as well as the interfacial tension Σ_{pd} between the external liquid phases must balance. We then obtain the relations

$$\begin{aligned} \hat{\Sigma}_{di} + \hat{\Sigma}_{pi}\cos\theta_i + \Sigma_{pd}\cos\theta_d &= 0, \\ \hat{\Sigma}_{di}\cos\theta_i + \hat{\Sigma}_{pi} + \Sigma_{pd}\cos\theta_p &= 0, \\ \hat{\Sigma}_{di}\cos\theta_d + \hat{\Sigma}_{pi}\cos\theta_p + \Sigma_{pd} &= 0, \end{aligned} \qquad \text{(S1)}$$

with $\theta_i + \theta_p + \theta_d = 2\pi$. Furthermore, we can define the intrinsic contact angle of the external PEG-rich phase with the membrane in an analogous way to Ref. [1] for outward budding. As shown in Fig. S3b, this angle satisfies the simple relation

$$\cos\theta_{in} = \frac{\hat{\Sigma}_{di} - \hat{\Sigma}_{pi}}{\Sigma_{pd}}. \qquad \text{(S2)}$$

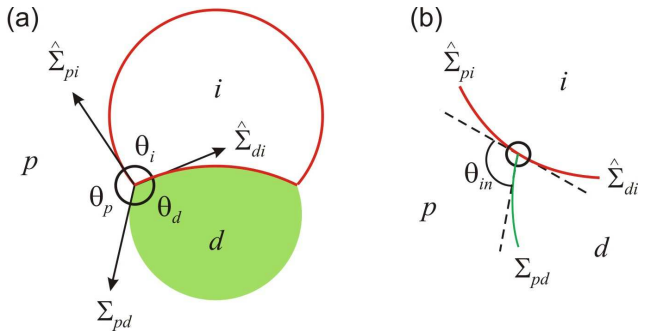

Figure S3. (a) Cross section of vesicles enclosing one droplet of interior phase *i* in contact with one exterior droplet of dextran-rich phase *d* (green) and the exterior bulk phase *p*. The thick red line represents the membrane. (b) Schematic illustration of the intrinsic contact angle of the external PEG-rich phase with the membrane. The three contact angles θ_i, θ_d, and θ_p and the three tensions $\hat{\Sigma}_{pi}$, Σ_{pd}, and $\hat{\Sigma}_{di}$ satisfy the three balance relations (S1).

Interfacial tension measurements: The bulk polymer solutions were prepared by mixing certain amount of PEG stock solution, dextran stock solution and water in 50 ml separatory funnels, respectively. The weight of each component was measured with a balance. The weight ratio of dextran and PEG was fixed to 0.55, as the one in the homogeneous polymer solution (2.22 wt% dextran and 4.05 wt% PEG) in all samples. The total weight in each funnel was around 60 g solution. The solutions were shaken by hand to make the polymers mix well. They were left at 24.2 ºC (room temperature with small fluctuations) for 4 to 5 days. Afterwards, the two phases were separated. The dextran-rich phase was taken out through the lower outlet, and the PEG-rich phase through the upper outlet

The interfacial tensions of the coexisting phases were measured at 24.2 ºC using a spinning drop tensiometer (SITE100SQ, Krüss). The density differences of the coexisting phases, which were needed to calculate the interfacial tension, were measured at 24.2 ºC with a density meter (DMA5000, Anton Paar).

Vesicle aspiration with micropipettes: The freshly formed vesicles containing 4.05 wt% PEG and 2.22 wt% dextran were diluted in the isotonic solution, and pre-deflated by adding the hypertonic solution (3.92 wt% PEG, 2.14 wt% dextran and 3.27 wt% sucrose) into the external medium stepwise. The increment in the osmolarity ratio r (see the main text for definition) was approximately 6.5% for each step, and the time interval between two steps was at least 15 minutes to avoid budding during deflation. At the end, the system was left over night to equilibrate. The deflated vesicles were carefully transferred into the working chamber. The micropipettes were pulled by a micropipette puller (P-97, Sutter Instrument Co.), and the tips shaped with a micro forge (MF-900, Narishige). The pipette inner diameters were typically ~20 μm. A pipette was inserted into the chamber from the top. To eliminate adhesion, the tip was pre-coated with lipids by breaking several vesicles. The opened side of the chamber was sealed with high viscous grease to avoid evaporation. Aspiration was realized by means of a hydrostatic pressure system with a motorized vertical stage (M-531.PD, Physik Instrumente). The system was left to equilibrate for about 3 minutes after each consecutive pressure change. Vesicle aspiration was observed from the side. All experiments were performed at room temperature.

The pipette tip was in contact with the membrane enclosing the PEG-rich phase, therefore the tension controlled via the pipette is $\hat{\Sigma}_{pe}$. It can be calculated from the following equation [2].

$$\hat{\Sigma}_{pe} = \frac{PR_{pip}}{2(1- R_{pip}/R_p)} \qquad \text{(S3)}$$

where P is the suction pressure, R_p is the radius of the PEG-rich phase, and R_{pip} is the radius of the spherical part of the vesicle inside the micropipette.

The change in the contact area between the dextran- and the PEG-rich phases corresponding to the measurement shown in Fig. 3 is given in Fig. S4. Similar measurements were performed on altogether four vesicles.

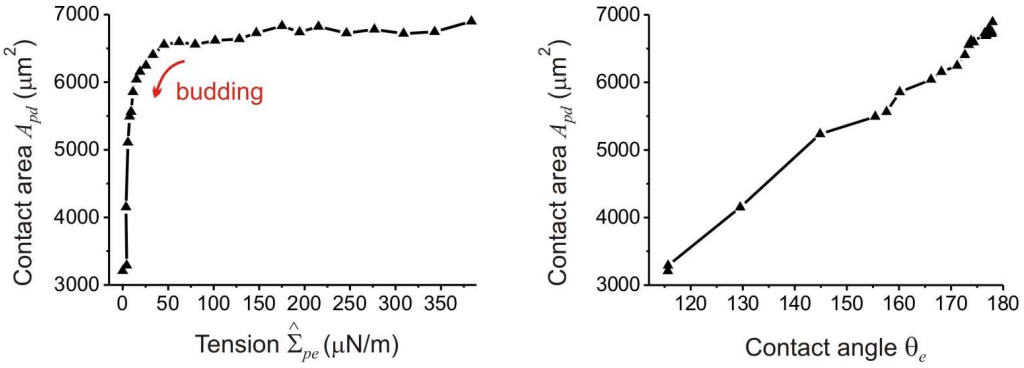

Figure S4. Change in the contact area A_{pd} for the vesicle in Fig. 3 in the main text as a function of the tension $\hat{\Sigma}_{pe}$ applied with a micropipette (left panel) and the same data as a function of the contact angle θ_e (right panel).

Derivation of Eq. (3) in the main text: In the limit where θ_e approaches π, we can write

$$\theta_e = \pi - \delta \qquad \text{(S4)}$$

where δ is a small parameter, $\delta \rightarrow 0$. Substituting (S4) into the relation $\theta_p + \theta_d + \theta_e = 2\pi$, we have

$$\theta_d = \pi + \delta - \theta_p \quad . \qquad \text{(S5)}$$

Thus,

$$\frac{\sin\theta_p - \sin\theta_d}{\sin\theta_e} = \frac{\sin\theta_p - \sin(\theta_p - \delta)}{\sin\delta} = \cos\theta_p + \sin\theta_p \tan\left(\frac{\delta}{2}\right) \approx \cos\theta_p + \frac{\delta}{2}\sin\theta_p . \qquad \text{(S6)}$$

Calculated vesicle shapes: In the main text, the budding process was analyzed using force balance arguments. The same conclusions can be obtained from a systematic theory that includes the membrane bending energy [1]. The experimental input parameters are the vesicle volume and area as well as the volume ratio of the PEG-rich and dextran-rich phases, which are estimated from the microscopy images. Given these constraints, one obtains a family of solutions corresponding to different local energy minima. Thus, the shape of the vesicle cannot be uniquely computed. However, identifying the experimentally

measurable property $\left(\hat{\Sigma}_{de} - \hat{\Sigma}_{pe}\right)/\Sigma_{pd}$ with the cosine of the intrinsic contact angle as in Eq. (4) in the main text, the vesicle shape can be uniquely predicted without any fitting parameter. The computed shapes are in excellent agreement with the vesicle images; see Fig. S5.

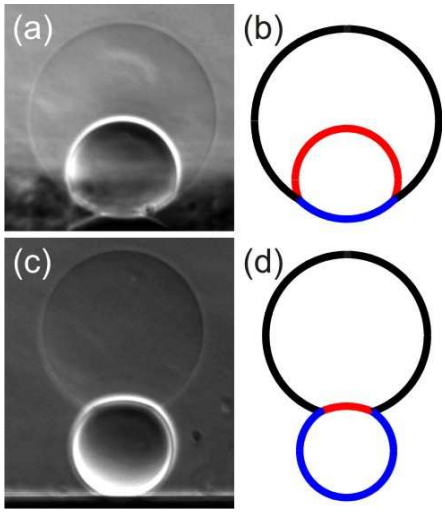

Figure S5. Comparison between vesicle images and theoretically calculated shapes. (a, c) Phase contrast images corresponding to the snapshots given in Fig. 1c,f in the main text. (b, d) computed cross-sections based on the theory discussed in [1].

Saturation of the tension $\hat{\Sigma}_{pe}$ at high osmolarity ratios: The tension $\hat{\Sigma}_{pe}$ saturates for high polymer concentration; see Fig. 2c in the main text. Because $\hat{\Sigma}_{pe}$ is governed by the membrane spontaneous curvature [3], we expect that the latter reaches saturation as well. One contribution to the spontaneous curvature arises from the different composition of the exterior solution and the two aqueous phases within the vesicles. For the systems studied here, the exterior solution contained PEG, dextran, and sucrose, whereas the interior PEG-rich and dextran-rich phases contained primarily PEG and dextran, respectively. The associated compositional asymmetry across the *pe* and *de* membranes leads to spontaneous or prefered curvatures m_{pe} and m_{de} of the two membrane segments. More precisely, these spontaneous curvatures reflect the different interactions between the membranes and the three molecular species [4,5].

If PEG molecules were adsorbed onto the membranes, for example, two layers of PEG would be formed on the two sides of the membranes, which would then prefer to curve away from the denser layer. In general, one expects to see competitive adsorption of several species such as PEG and dextran. In the latter case, the spontaneous curvature would saturate for high polymer concentrations if the interior and exterior membrane surfaces became completely covered with PEG and dextran and the corresponding adsorption layers differed in their composition.

As shown in Fig. S6, the PEG-rich phase contains essentially no dextran for large polymer concentrations. Therefore, in this concentration regime, the adsorption layer at the interior surface of the *pe* membrane would consist only of PEG whereas the adsorption layer at the exterior surface of the *pe* membrane would consist of both PEG and dextran. It remains to be seen if such a molecular mechanism can be corroborated by further experimental studies.

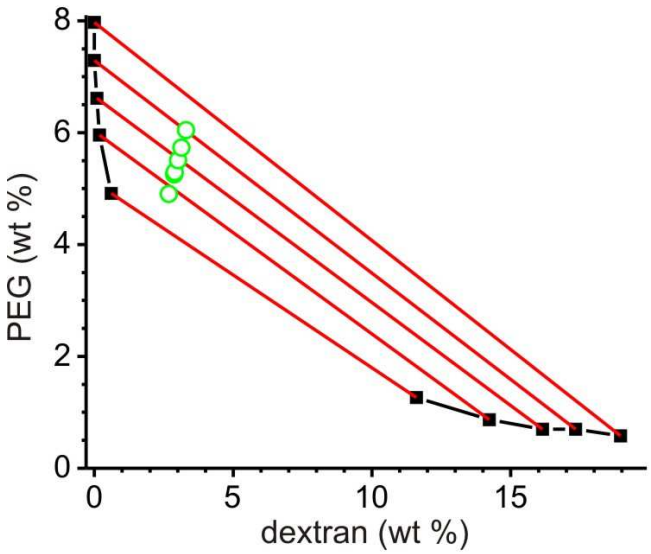

Figure S6. Coexistence curve and tie lines of dextran and PEG aqueous solutions as measured with gel permeation chromatography at 23 ºC. The black curves are a guide to the eyes. The red lines illustrate the tie lines. At high polymer concentrations, no dextran is detected in the PEG-rich phase. The green open circles indicate the composition of polymer solutions explored in this work.

REFERENCES

(1) Kusumaatmaja, H.; Li, Y.; Dimova, R.; Lipowsky, R. *Physical Review Letters* 2009, *103*, 238103.

(2) Evans, E.; Rawicz, W. *Physical Review Letters* 1990, *64*, 2094.

(3) Li, Y.; Lipowsky, R.; Dimova, R. *Proceedings of the National Academy of Sciences of the United States of America* 2011, *108*, 4731.

(4) Lipowsky, R.; Dobereiner, H. G. *Europhysics Letters* 1998, *43*, 219.

(5) Breidenich, M.; Netz, R. R.; Lipowsky, R. *Molecular Physics* 2005, *103*, 3169.